Progress In Electromagnetics Research C, Vol. 38, 67–78, 2013

DESIGN AND INVESTIGATION OF A DUAL-BAND ANNULAR RING SLOT ANTENNA FOR AIRCRAFT APPLICATIONS

Li Sun*, Bao-Hua Sun, Guan-Xi Zhang, Dan Cao, and Bin Fan

National Key Laboratory of Science and Technology on Antennas and Microwaves, Xidian University, Xi'an, Shaanxi 710071, China

Abstract—A novel dual-band annular ring slot antenna is investigated. The antenna consists of a center-fed circular microstrip patch antenna with a coupled annular ring. And it is shorted concentrically with a set of conductive vias. By adjusting the parameters of the antenna, the dual resonant frequencies for two modes (TM_{01} and TM_{02} modes) are achieved. The antenna is fabricated and tested. Results show that the proposed antenna with height of $0.0217\lambda_0$ can provide gains of 3.01 dBi at 2.6 GHz (the receiving frequency) and 5.74 dBi at 2.95 GHz (the transmitting frequency). Good agreement between the measurement and simulation for the return loss and radiation patterns is achieved. The proposed antenna has dual-band characteristics, simple structure, low profile, and omni-directional azimuth radiation pattern. It is suitable for aircraft both receiving and transmitting signals and frequency division duplex (FDD) applications.

1. INTRODUCTION

The rapid progress in aircraft communication requires the development of lightweight, low-profile, flush-mounted and single-feed antennas. Also, it is highly desirable to integrate several RF modules for different frequencies into one piece of equipment. Annular ring slot antennas are widely used as the installation to an aircraft since they have the advantages of simple structure, low profile, and omni-directional azimuth radiation pattern.

In recent years, many annular ring slot antennas have been developed for dual-frequency operations [1–13], and several of methods

Received 23 January 2013, Accepted 14 March 2013, Scheduled 15 March 2013

* Corresponding author: Li Sun (lisun@stu.xidian.edu.cn).

have been used to create antenna with dual-band characteristic. One of the typical methods is to introduce another concentric annular-ring slot [1–6]. However, in order to obtain the dual-band input impedance matching, some other structures should be embedded into the antenna, such as circular photonic bandgap (PBG) structures [3], tree-shaped coupling strip with branches [5] and a cross-slot [6]. There are many other methods to generate dual-band function, such as using triplate feed [7, 8], introducing a back-patch [9], utilizing pin diodes [10], changing the compact annular ring slot structure [11–13]. All these antennas provide a better impedance match but have some drawbacks of comparatively complex structures [3, 6–8, 10, 13], high profile [7, 8], and a large ground plane [9, 12]. On the other hand, there are many classic papers introducing the basic analysis methods of the printed and slot antennas [14–17], and the operation modes analysis using cavity model of annular ring antennas are also introduced [5, 7, 8, 18], which provide a physical insight for understanding the behavior of the antennas. Besides, the antennas with similar structure but different operation modes compared with annular ring slot antennas are introduced [18, 19].

In this paper, we propose a new dual-band annular ring slot antenna. The antenna is based on an annular ring slot antenna that is shorted concentrically with a set of conductive vias. The annular ring slot antenna presents a novel frequency characteristic which can achieve dual-band characteristics. This type of antenna can produce a monopole-like radiation pattern with low profile. We analyze the novel dual-band annular ring slot antenna using a cavity model. The cavity model analysis distinguishes clearly each resonating mode in the antenna and gives a better understanding of the novel frequency characteristics. The antenna is designed and fabricated. The geometry of the antenna and its novel characteristics are discussed in Section 2. Section 3 presents the optimized design and its simulation results for validating the novel characteristic. And Section 4 presents a parametric study of the proposed antenna and explains their effects. For our specific application scenario, a prototype operates at 2.6 GHz (the receiving frequency) and 2.95 GHz (the transmitting frequency) is designed, fabricated and tested. Experimental results for the return losses and radiation patterns are presents in Section 5.

2. ANTENNA STRUCTURE AND CAVITY MODEL ANALYSIS

The geometry of the annular ring slot antenna is shown in Figure 1. The circular patch has a radius of R. The radius of the concentric

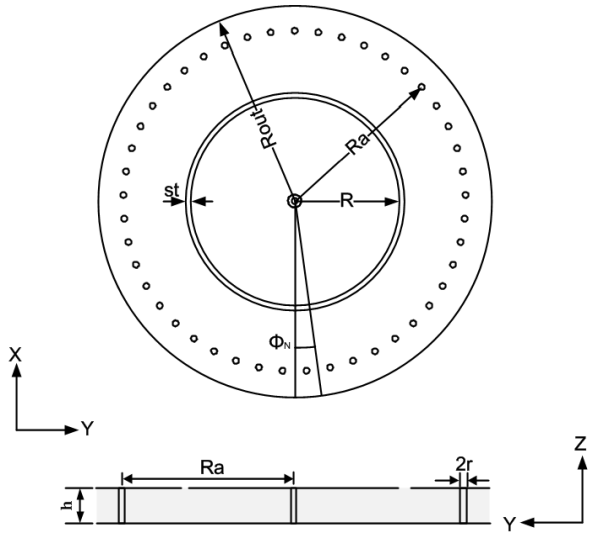

Figure 1. Geometry of the annular ring slot antenna. The number of conductive vias is N. $\phi = 2\pi/N$.

annular-ring patch is R_{out}. The width of the slot is st. The annular ring slot antenna is shorted concentrically with a set of N conductive vias. Each via has a radius of r. The center of each via is at a distance of R_a from the center of the circular path. The antenna is fed at the center by a coaxial probe with an SMA connector which is placed underneath the ground plane.

Keeping the other parameters constant, Figure 2 shows how the resonant frequencies vary with the radius circular patch R. As the radius of the circular patch increases from 20 mm to 50 mm, resonant frequencies curves 1, 2, 3 decrease while 4, 5, 6 increase.

Suppose the height h of the annular ring slot antenna in Figure 1 is very small when compared with the wavelength λ_0 in free space or the radius of the top patch. Then a cavity model can be used to analyze the annular ring slot antenna for the TM modes [20]. In this analysis, the feeding line is not considered. Here, we only consider the $\mathrm{TM}_{0\,\mathrm{m}}$ modes in the annular ring slot antenna, since only the $\mathrm{TM}_{0\,\mathrm{m}}$ modes can produce a monopole like radiation pattern. For the $\mathrm{TM}_{0\,\mathrm{m}}$ modes, the field inside the structure must be symmetric about the z axis. As shown in Figure 1, the N conductive vias are supposed to be placed symmetrically around the z axis. Due to the symmetric property of the structure in Figure 1, the interface between two sectors should be a magnetic plane for the $\mathrm{TM}_{0\,\mathrm{m}}$ modes. Besides, the center

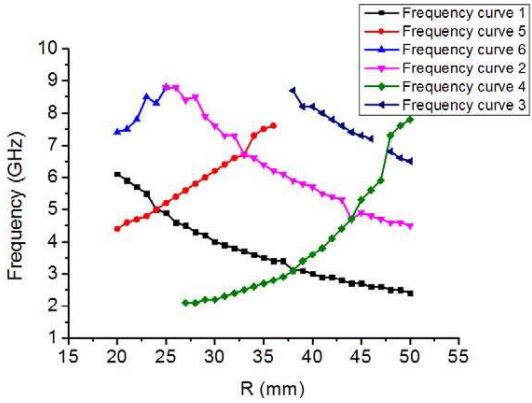

Figure 2. The results of the radiation frequencies change with the variation of the R.

plane of each sector with an angle of $\phi = 2\pi/N$ should be a perfect magnetic symmetric plane. Thus, the characteristic shown in Figure 2 is analyzed using the $TM_{0\,m}$ modes.

Previously, the modes in a center-fed circular patch-ring antenna were analyzed using a cavity mode [18]. If the radius of the patch increases, the resonant frequency for TM_{02} mode decreases. It is concluded that the frequency curve 1 is composed of the frequencies operating at TM_{02} mode, which is the basic mode of the frequencies decreasing with the increased R. The frequency curve 2 is composed of the frequencies operating at higher order modes mixing TM_{02} mode and TM_{04} mode (The electric field is not shown here). The frequency curve 6 is composed of the frequencies operating at higher order modes mixing TM_{02} mode, TM_{04} mode and other higher order mode which is more complicated. On the other hand, according to [15], when the circular patch is not shorted with conductive via ($N = 0$), the resonant frequency for the lowest mode (TM_{01} modes) is zero. Therefore, the introduced shorting-vias generate a non-zero resonant frequency for the TM_{01} mode. The resonant frequencies for the TM_{01} modes increase with the increasing value of R due to the coupling between the annular ring slot and the shorting-vias. Thus, the frequency curve 4 is composed of the frequencies operating at TM_{01} mode. The frequency curve 5 is composed of the frequencies operating at higher order mode mixing TM_{01} mode and TM_{03} mode. The frequency curve 6 is composed of the frequencies operating at higher order modes mixing TM_{01} mode, TM_{03} mode and other higher order mode which is more complicated.

3. VALIDATING THE NOVEL CHARACTERISTIC

For validating the novel characteristic, the annular ring slot antenna is simulated. All design parameters are concluded in Table 1. The numerical analysis and geometry refinement of the proposed structure are performed by using ANSYS HFSS 14.0 software. Figure 3 shows the return loss of the proposed antenna. Two resonant frequencies are obtained by using the novel characteristics shown in Figure 1.

Table 1. Geometrical parameters of the proposed antenna.

Parameters	R	R_a	R_{out}	st	r	h	N
Value	41.5 mm	57.1 mm	64 mm	2.2 mm	1 mm	2.5 mm	45

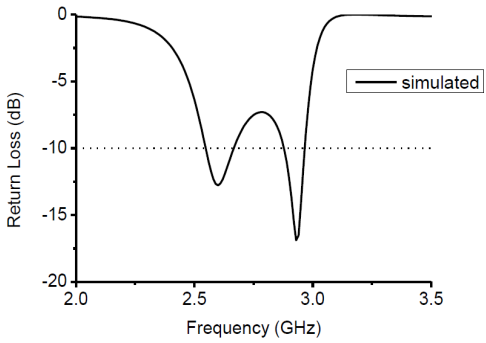

Figure 3. Simulated return loss of the antenna.

The electric fields for two resonant frequencies are shown in Figures 4 and 5, respectively. It is seen that the electric fields for the two resonant frequencies are similar, except two significant differences. One is that the electric fields for the lower frequency have almost the same directions ignoring the slight interference of the annular slot, while the electric fields for the higher frequencies have opposite directions at the two sides of the annular slot. The other different is that the electric fields at the concentric annular-ring patch are weak for the lower frequency while quite strong for the higher frequency. Because the TM_{01} mode has the electric fields having the same directions while the TM_{02} mode has the electric fields having opposite directions, it is concluded that the lower frequency works at TM_{01} mode while the higher frequency works at TM_{02} mode. While not shown here, the electric field for the TM_{02} mode is much weaker at the concentric annular-ring patch than the TM_{02} mode for

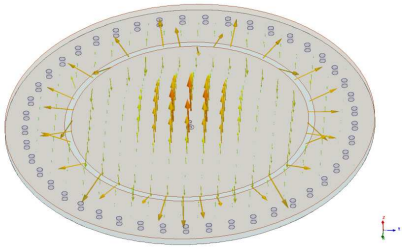

Figure 4. Electric fields for the TM_{01} mode of the cavity model for the via-shorted annular ring slot antenna. The resonant frequency is 2.60 GHz.

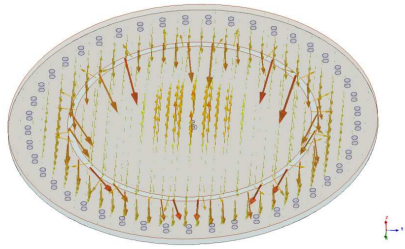

Figure 5. Electric fields for the TM_{02} mode of the cavity model for the via-shorted annular ring slot antenna. The resonant frequency is 2.94 GHz.

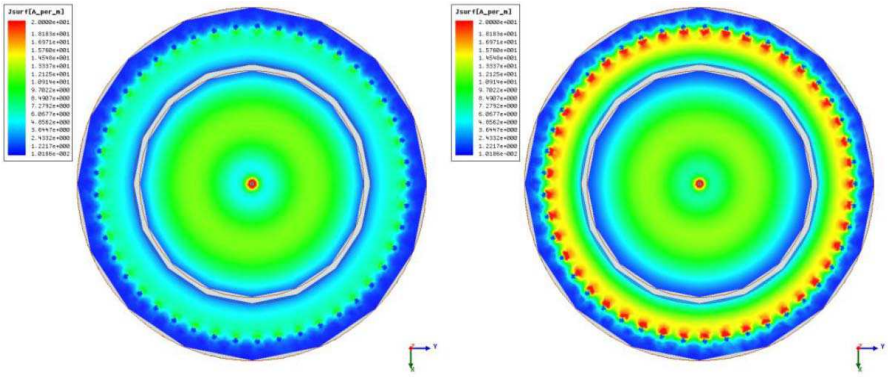

(a) (b)

Figure 6. Current distributions on the top surface of the antenna, (a) at 2.60 GHz, (b) at 2.94 GHz.

the cylindrical cavity without shorting-vias [14]. The shorting-vias not only generate the TM_{01} mode but also enhance the TM_{02} mode. The surface current distributions of the antenna at 2.60 GHz and 2.94 GHz are shown in Figure 6 for validating the correct of the analysis.

4. PARAMETERIC STUDY AND DISCUSSION

From the previous sections, it is noticed that the introduced conductive vias have much influence on the antenna operation modes (TM_{01} and TM_{02} modes). And several parameters about the shorting-vias such as

the position, the radius, and the number of the shorting-vias affect the resonant frequencies and the matching of the antenna. In this section, we will demonstrate the effect of each of these parameters.

Figure 7 shows the return loss of the proposed antenna for different values of the position R_a. The other parameters of the antenna are: $R = 41.4\,\text{mm}$, $st = 2.2\,\text{mm}$, $h = 2.5\,\text{mm}$, $R_{out} = 64\,\text{mm}$, $r = 1\,\text{mm}$, and $N = 45$. It is observed that when the value of R_a increases, the value of resonant frequency for the TM_{02} mode decreases while the value of resonant frequency for the TM_{01} mode changes slightly. On the other hand, the return losses of both TM_{01} mode and TM_{02} mode shift dramatically. Matching for the TM_{01} mode improves as R_a decreases while matching for the TM_{02} mode is best when R_a is equal to 56.8 mm. As analyzed above, the resonant frequency for the TM_{02} modes decreases due to the increase of the resonant current path (R_a). On the other hand, it can be seen from the figure that there is only slight change of the resonant frequency for the TM_{01} mode since the parameters R and st are unchanged, but the return loss of the resonant frequency for the TM_{01} mode increases with the increasing R_a.

The return loss of the proposed antenna with different values of the radius r is shown in Figure 8, while other parameters are: $R = 41.4\,\text{mm}$, $st = 2.2\,\text{mm}$, $h = 2.5\,\text{mm}$, $R_{out} = 64\,\text{mm}$, $R_a = 57.1\,\text{mm}$, and $N = 45$. The results shown in Figure 8 are similar to the results shown in Figure 7 except the different parameter. It is concluded from Figures 7 and 8 that with the variation of R_a and r, the resonant frequency for the TM_{01} mode changes slightly. By changing the position and the radius of the shorting-vias, the resonant frequency for the TM_{02} mode will change with the almost constant value of the resonant frequency for the TM_{01} mode.

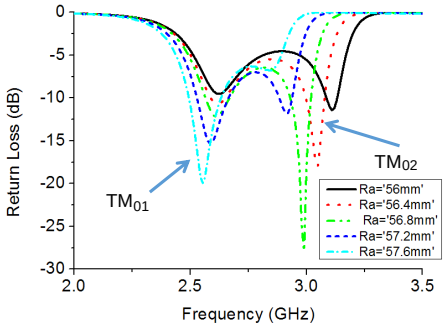

Figure 7. Return loss for the proposed antenna for different values of R_a.

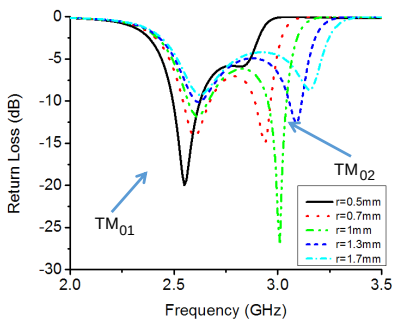

Figure 8. Return loss for the proposed antenna for different values of r.

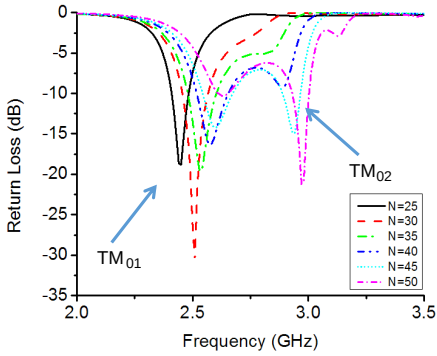

Figure 9. Return loss for the proposed antenna for different values of N.

Figure 9 shows the return loss of the proposed antenna for different values of the number of the shorting-vias N with the parameters: $R = 41.4\,\text{mm}$, $st = 2.2\,\text{mm}$, $h = 2.5\,\text{mm}$, $R_{out} = 64\,\text{mm}$, $R_a = 57.1\,\text{mm}$, and $a = 1\,\text{mm}$. It can be noticed that the dual-band characteristic can achieve only when the number of the shorting-vias N is enough large. Though the introduced shorting-vias generate the TM_{01} mode, the TM_{01} mode becomes weaker while the inherent mode of the annular ring slot antenna (TM_{02} mode) becomes stronger with the larger N. Hence, it seems that the TM_{02} mode in the concentrically shorted annular ring slot antenna is a perturbed mode of the TM_{02} mode in the corresponding annular ring slot antenna without shorting-vias. By optimizing the parameter N, a good separation of TM_{01} mode and TM_{02} mode can be achieved, and dual-band characteristic is obtained.

5. EXPERIMENTAL RESULTS

In this section, an annular ring slot antenna with dual-band and very low profile is fabricated. The antenna is printed on a Teflon dielectric substrate with the dielectric constant (ε_r) of 2.65, the loss tangent ($\tan\delta$) of 0.001 and the substrate thickness of 2.5 mm (about $0.0217\lambda_0$ at 2.6 GHz). It is fed by a coaxial transmission line with $50\,\Omega$ at the center. Figure 10 shows a photo of the fabricated antenna.

It is not so easy to match an annual ring slot antenna (fed at the center) if the antenna works in a single mode (TM_{02} mode). The reflection coefficient for an annular ring slot antenna without shorting-vias is shown in Figure 11. Figure 11 shows that the antenna has a high reflection coefficient, meaning poor impedance match. In order to match the annular ring slot antenna and achieve dual-band, another

(a) (b)

Figure 10. Photograph of the proposed antenna. (a) Top view. (b) Back view.

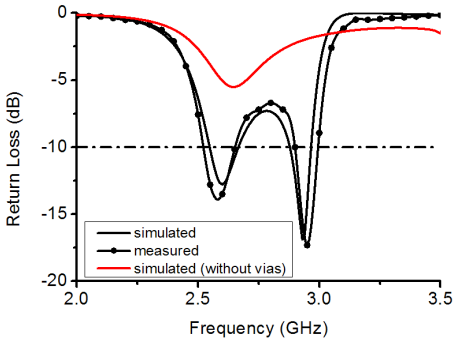

Figure 11. Measured and simulated return loss of the proposed antenna.

mode (TM_{02} mode) is introduced to couple the TM_{02} mode. As analyzed above, the TM_{01} mode can be generated by adding shorting-vias. Therefore, an annular ring slot antenna working in TM_{01} and TM_{02} modes can be designed, with the geometry shown in Figure 1 and the photo of optimized antenna is shown in Figure 10.

Simulated and measured results for the return loss are shown in Figure 11. Measured results agree well with the simulated results, as shown in Figure 11. The discrepancy is mainly due to the insert loss of the connector and manufacturing tolerance.

The simulated and measured radiation patterns for TM_{01} mode (at 2.6 GHz) and TM_{02} mode (at 2.95 GHz) are shown in Figures 12(a) and (b), respectively. The measured gain of the proposed antenna is 3.01 dBi at 2.6 GHz and 5.74 dBi at 2.95 GHz. Measured results agree very well with simulated results. Results also show that the patterns

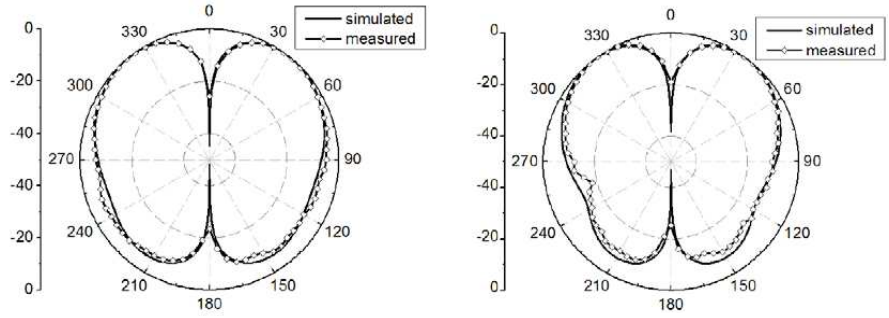

Figure 12. Measured and simulated elevation radiation patterns at (a) 2.6 GHz, (b) 2.95 GHz.

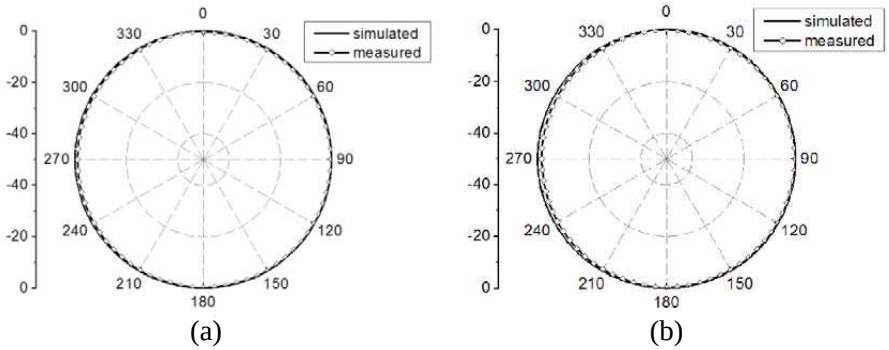

Figure 13. Measured and simulated azimuth radiation patterns at (a) 2.6 GHz, (b) 2.95 GHz.

for two modes are similar, so the radiation pattern should be stable at two bands.

The simulated and measured far-field azimuth radiation patterns for 2.6 GHz and 2.95 GHz are plotted in Figures 13(a) and (b). It shows that the proposed antenna produces omni-directional azimuth radiation patterns.

6. CONCLUSION

A novel annular ring slot antenna is proposed and analyzed. The antenna is based on an annular ring slot antenna that is concentrically shorted with a set of conductive vias. The modes in this type of antenna are analyzed using a cavity model. The introduced shorting-vias not only generate a new mode (TM_{01} mode), but also provides a

new way for the design of an annular ring slot antenna with dual-band.

The novel dual-band annular ring slot antenna with very low profile is designed. The antenna works in TM_{01} and TM_{02} modes depending on the frequency. Results show that the proposed antenna with $0.0217\lambda_0$ can provide gains of 3.01 dBi at 2.6 GHz and 5.74 dBi at 2.95 GHz. The proposed antenna exhibits dual-band, simple structure, low-profile and omni-directional azimuth radiation pattern, which indicates its promising use in the aircraft wireless communication.

REFERENCES

1. Chen, J.-S., "Dual-frequency annual-ring slot antennas fed by CPW feed and microstrip line feed," *IEEE Transactions on Antennas and Propagation*, Vol. 53, 569–571, 2005.
2. Chen, J.-S., "Multi-frequency characteristics of annual-ring slot antennas," *Microwave and Optical Technology Letters*, Vol. 38, 506–511, 2003.
3. Sabri, H. and Z. Atlasbaf, "Two novel compact triple-band microstrip annular-ring slot antenna for PCS-1900 and WLAN applications," *Progress In Electromagnetics Research Letters*, Vol. 5, 87–98, 2008.
4. Chen, Q., H.-L. Zheng, J.-H. Hu, and S.-G. Jiang, "Design of CPW-fed dual-band circularly-polarized annular slot antenna with two perturbation strips," *Progress In Electromagnetics Research C*, Vol. 28, 195–207, 2012.
5. Liu, J.-C., B.-H. Zeng, C.-Y. Wu, and D.-C. Chang, "Double-ring slot antenna with tree-shaped coupling strip for WLAN 2.4/5-GHz dual-band applications," *Microwave and Optical Technology Letters*, Vol. 47, 347–349, 2005.
6. Bao, X.-L. and M.-J. Ammann, "Compact concentric annular-ring patch antenna for triple-frequency operation," *Electronics Letters*, Vol. 42, 1129–1130, 2006.
7. Batchelor, J.-C. and R.-J. Langley, "Microstrip annular ring slot antennas for mobile applications," *Electronics Letters*, Vol. 32, 1635–1636, 1996.
8. Chen, C. L. and N. G. Alexopoulos, "Triplate-fed arbitrarily-shaped annular ring slot antennas," *IEEE Antennas and Propagation Society International Symposium*, Vol. 4, 2070–2072, 2005.
9. Chen, J.-S. and H.-D. Chen, "Dual-band characteristics of annular-ring slot antenna with circular back-patch," *Electronics Letters*, Vol. 39, 487–488, 2003.

10. Nikolaou, S. and R. Bairavasubramanian, "Pattern and frequency reconfigurable annular slot antenna using PIN diodes," *IEEE Transactions on Antennas and Propagation*, Vol. 54, 439–448, 2006.
11. Sze, J.-Y., C.-G. Hsu, and S.-C. Hsu, "Design of a compact dual-band annular-ring slot antenna," *IEEE Antennas and Wireless Propagation Letters*, Vol. 6, 423–426, 2007.
12. Chiang, M.-J., T.-F. Hung, J.-Y. Sze, and S.-S. Bor, "Miniaturized dual-band CPW-fed annular slot antenna design with arc-shaped tuning stub," *IEEE Transactions on Antennas and Propagation*, Vol. 58, 3710–3715, 2010.
13. Sze, J.-Y., T.-H. Hu, and T.-J. Chen, "Compact dual-band annular-ring slot antenna with meandered grounded strip," *Progress In Electromagnetics Research*, Vol. 95, 299–308, 2009.
14. Lee, J. Y., T. S. Horng, and N. G. Alexopoulos, "Analysis of cavity-backed aperture and antennas with a dielectric overlay," *IEEE Transactions on Antennas and Propagation*, Vol. 42, 1556–1562, 1994.
15. Liu, H. C., T. S. Horng, and N. G. Alexopoulos, "Radiation of printed antennas with co-planar waveguide feed," *IEEE Transactions on Antennas and Propagation*, Vol. 43, 1513–1148, 1995.
16. Chen, C. L., W. E. McKinzie, and N. G. Alexopoulos, "Stripline-fed arbitrarily shaped printed-aperture antennas," *IEEE Transactions on Antennas and Propagation*, Vol. 45, 1186–1198, 1997.
17. Chen, C. and N. G. Alexopoulos, "Modeling microstrip line fed slot antennas with arbitrary shape," *Electromagnetics*, Vol. 15, 567–586, 1995.
18. Asem, A.-Z., F. Yang, and A. Kishk, "A broadband center-fed circular patch-ring antenna with a monopole like radiation pattern," *IEEE Transactions on Antennas and Propagation*, Vol. 57, 789–792, 2009.
19. Boutayeb, H. and T. A.Denidni, "Gain enhancement of a microstrip patch antenna using a cylindrical electromagnetic crystal substrate," *IEEE Transactions on Antennas and Propagation*, Vol. 55, 3140–3145, 2007.
20. Garg, R., P. Bhartia, I. Bahl, and A. Ittipiboon, *Microstrip Antenna Design Handbook,* Artech House, Norwood, MA, 2001.